ORIGINAL ARTICLE
Nephrology

JKMS

http://dx.doi.org/10.3346/jkms.2016.31.9.1403 • J Korean Med Sci 2016; 31: 1403-1412

Renoprotective Effects of a Highly Selective A3 Adenosine Receptor Antagonist in a Mouse Model of Adriamycin-induced Nephropathy

Hye Sook Min,[1]* Jin Joo Cha,[1]* Kitae Kim,[1] Jung Eun Kim,[1] Jung Yeon Ghee,[1] Hyunwook Kim,[2] Ji Eun Lee,[2] Jee-Young Han,[3] Lak Shin Jeong,[4] Dae Ryong Cha,[1] and Young Sun Kang[1]

[1]Department of Nephrology, Korea University Ansan Hospital, Ansan, Korea; [2]Department of Nephrology, Wonkwang University Sanbon Hospital, Gunpo, Korea; [3]Department of Pathology, Inha University Medical College, Incheon, Korea; [4]Department of Pharmacy, College of Pharmacy, Seoul National University, Seoul, Korea

*Hye Sook Min and Jin Joo Cha contributed equally to this work.

Received: 30 January 2016
Accepted: 13 May 2016

Address for Correspondence:
Young Sun Kang, MD
Department of Nephrology, Korea University Ansan Hospital, 123 Jeokgeum-ro, Danwon-gu, Ansan 15355, Korea
E-mail: starch70@korea.ac.kr

Funding: This research was supported by Korea University Grant in 2015 (Q1508671).

The concentration of adenosine in the normal kidney increases markedly during renal hypoxia, ischemia, and inflammation. A recent study reported that an A3 adenosine receptor (A3AR) antagonist attenuated the progression of renal fibrosis. The adriamycin (ADX)-induced nephropathy model induces podocyte injury, which results in severe proteinuria and progressive glomerulosclerosis. In this study, we investigated the preventive effect of a highly selective A3AR antagonist (LJ1888) in ADX-induced nephropathy. Three groups of six-week-old Balb/c mice were treated with ADX (11 mg/kg) for four weeks and LJ1888 (10 mg/kg) for two weeks as following: 1) control; 2) ADX; and 3) ADX + LJ1888. ADX treatment decreased body weight without a change in water and food intake, but this was ameliorated by LJ1888 treatment. Interestingly, LJ1888 lowered plasma creatinine level, proteinuria, and albuminuria, which had increased during ADX treatment. Furthermore, LJ1888 inhibited urinary nephrin excretion as a podocyte injury marker, and urine 8-isoprostane and kidney lipid peroxide concentration, which are markers of oxidative stress, increased after injection of ADX. ADX also induced the activation of proinflammatory and profibrotic molecules such as TGF-β1, MCP-1, PAI-1, type IV collagen, NF-κB, NOX4, TLR4, TNFα, IL-1β, and IFN-γ, but they were remarkably suppressed after LJ1888 treatment. In conclusion, our results suggest that LJ1888 has a renoprotective effect in ADX-induced nephropathy, which might be associated with podocyte injury through oxidative stress. Therefore, LJ1888, a selective A3AR antagonist, could be considered as a potential therapeutic agent in renal glomerular diseases which include podocyte injury and proteinuria.

Keywords: Adriamycin; Nephropathy; Adenosine Receptor Antagonist; Mouse Model

INTRODUCTION

Adenosine is well known to have a cell protective effect in stressful situations, such as ischemia, hypoxia, and inflammation (1). It is released from metabolically active cells into the extracellular space and is produced by the breakdown of released adenosine triphosphate (ATP). While the concentration of extracellular adenosine is about 300 nM in normal cells (2), its concentrations rapidly exceed 1 μM in cells undergoing damage (3). Adenosine's regulation of tissue function is mediated through activation of a family of 4 G-protein coupled receptors, which includes the A1, A2a, A2b, and A3 adenosine receptors (AR). Concentrations of extracellular adenosine vary widely depending on external factors and the degree of stress, tissue types, and activation levels of the 4 adenosine receptors (4). Previous studies investigating the role of adenosine have focused on the agonists and antagonists of adenosine receptors instead of adenosine itself, because of the limitation of its very short half-life (5).

The A3 adenosine receptor (A3AR) has been detected in a wide variety of tissues. A3AR was highly expressed in the testis, but was less likely to be expressed in the lungs, kidney, heart, and central nervous system. Interestingly, inflammatory and cancer cells possess higher A3AR content than other adenosine receptor subtypes. A3AR is able to play a different roles under ischemic conditions, where it shows pro/anti-inflammatory, cellular proliferation/death, and pro/antitumoral effects depending on different pathophysiological environments (6). Previous studies demonstrated that inhibition of A3AR leads to kidney protection in ischemia-reperfusion injury (7) and myoglobinuria-induced injury (8). A recent study reported that A3AR antagonist ameliorates the progression of tubulointerstitial fibrosis in a unilateral ureteral obstruction (UUO) mice model (9).

Few reports have described the expression and distribution of adenosine receptor subtypes in the kidney and the role of A3AR and A3AR antagonists in kidney injury. A new A3AR antagonist (LJ1888) may be a powerful, highly selective, species-

© 2016 The Korean Academy of Medical Sciences.
This is an Open Access article distributed under the terms of the Creative Commons Attribution Non-Commercial License (http://creativecommons.org/licenses/by-nc/4.0) which permits unrestricted non-commercial use, distribution, and reproduction in any medium, provided the original work is properly cited.

pISSN 1011-8934
eISSN 1598-6357

independent, and orally available agent (10). However, there is rare data for the role of A3AR in glomerular kidney injury. The aim of this study was to investigate the mechanism and renoprotective effects of the highly selective A3AR antagonist (LJ1888) in adriamycin (ADX)-induced nephropathy.

MATERIALS AND METHODS

Experimental animals

All 6-week-old Balb/c male mice weighing 22-24 g were purchased from RaonBio Co. (Yongin, Korea). They were randomly assigned to three groups: control (n = 5); ADX injection (n = 10); or administration of LJ1888 after ADX injection (n = 10). Mice received a single tail vein injection of ADX diluted with 0.9% saline to a final dose of 11 mg/kg. Control mice received the same volume of isotonic saline. Four weeks after ADX injection, mice drank water mixed with 10 mg/kg per day of LJ1888 (Lee et al. [9] College of Pharmacy, Ewha Womans University, Seoul, Korea) for two weeks as previously described. All mice were provided with a standard diet and water, and were maintained at constant temperature (23°C ± 2°C) and humidity (55% ± 5%) with a 12-hour light/dark cycle. Daily food intake was monitored at regular intervals to confirm drug administration. Plasma creatinine level was determined using high-performance liquid chromatography. To determine urinary protein, albumin, and nephrin excretion, mice were caged individually and a 24-hour urine sample was collected at baseline, two, four and six weeks. Urinary albumin concentrations were determined with a competitive enzyme linked immunosorbent assay (ELISA) kit (ALPCO, Westlake, OH, USA). Urinary protein concentrations were determined by colorimetric detection using bicinchoninic acid (Pierce BCA protein Assay Kit, Pierce Biotech. Inc., Rockford, IL, USA). Urinary nephrin measurement was performed with the commercially available ELISA kit (Exocell, Philadelphia, PA, USA). The urinary 8-isoprostane level was measured using an ELISA kit (Cayman Chemical, Ann Arbor, MI, USA). The extent of peroxidative reaction in the kidney tissue was determined by direct measurement of lipid hydroperoxides (LPO) using an LPO assay kit (Cayman Chemical), as described previously (11). Mice were sacrificed under anesthesia with intraperitoneal injections of sodium pentobarbital (50 mg/kg). Their heart, epididymal fat, liver, and kidney tissues were extracted and subsequently snap-frozen in liquid nitrogen.

Analysis of gene expression by real-time quantitative polymerase chain reaction

We extracted total RNA from experimental cells using the Trizol reagent. Primers were designed for their respective gene sequences using the Primer 3 software, and the secondary structures of the templates were examined and excluded using the mfold program (Supplementary Table 1). Quantitative gene expression was performed using a Light Cycler 1.5 system (Roche Diagnostics Corporation, Indianapolis, IN, USA) using SYBR Green technology. In 96-well real-time polymerase chain reaction (PCR) plates, 10 μL SYBR Green master mix was added to 1 μL of RNA (corresponding to 50 ng of total RNA) and 900 nM of forward and reverse primers for a total reaction volume of 20 μL. Real-time reverse transcriptase PCR was performed for 10 minutes at 50°C and for 5 minutes at 95°C. Thirty PCR cycles of denaturation for 10 seconds at 95°C and annealing with extension for 30 seconds at 60°C were then conducted. Gene level ratios relative to β-actin (relative gene expression number) were calculated by subtracting the threshold cycle number of the target gene from that of β-actin and squaring this difference. We evaluated the specificity of each PCR product using melting curve analysis, followed by agarose gel electrophoresis.

Protein extraction and western blot analysis

Nuclear and cytoplasmic proteins were extracted from renal cortical tissues and cells using a commercial nuclear extraction kit according to the manufacturer's instructions (Active Motif, Carlsbad, CA, USA). Protein concentration was determined using the bicinchoninic acid method (Pierce Pharmaceuticals). For western blotting, 40 μg protein was electrophoresed on a 10% SDS-PAGE mini-gel. Proteins were transferred onto a polyvinylidene difluoride membrane, and the membrane was hybridized in blocking buffer overnight at 4°C with mouse monoclonal anti-nuclear factor (NF)-κB p65 antibody (1:1,000; Cell Signaling Technology, Danvers, MA, USA), rabbit polyclonal anti-transforming growth factor (TGF)-β1 antibody (1:200; Santa Cruz Biotechnology, Santa Cruz, CA, USA), rabbit polyclonal anti-nicotinamide adenine dinucleotide phosphate (NADPH) oxidase 4 (NOX4) antibody (1:500; Novus Biologicals, Littleton, CO, USA) and goat polyclonal anti-toll-like receptor 4 (TLR4) antibody (1:500; Santa Cruz Biotechnology). The membrane was subsequently incubated with horseradish peroxidase-conjugated secondary antibody (1:1,000 dilution) for 60 minutes at room temperature. We detected the specific signals using an enhanced chemiluminescence method (Amersham, Buckinghamshire, UK).

Histological examination and immunohistochemistry

Kidney samples were fixed in 10% buffered formalin and embedded in paraffin. Kidney tissue was cut into 4-μm-thick slices and stained with periodic acid Schiff (PAS), Masson's trichrome, and sirius red staining. Macrophage infiltration was detected by rat anti-mouse F4/80 antibody (1:2,000; Serotec, Raleigh, NC, USA) and incubated at room temperature for 1 hour, followed by use of the Envision kit (Dako, Carpinteria, CA, USA). To perform immunohistochemical staining for type I collagen, TGFβ1, and α-smooth muscle actin (SMA), kidney sections were transferred to a 10 mM/L citrate buffer solution adjusted to a pH of

 http://dx.doi.org/10.3346/jkms.2016.31.9.1403

6.0. Thereafter, sections were microwaved for 10–20 minutes to retrieve antigens for TGFβ1 and α-SMA, or treated with trypsin (Sigma, St. Louis, MO, USA) for 30 minutes at 37°C for type I collagen and type IV collagen. To block endogenous peroxidase activity, 3.0% H_2O_2 in methanol was applied for 20 minutes, followed by incubation at room temperature for 60 minutes with 3% BSA/3% normal goat serum. Slides were incubated overnight at 4°C with rabbit polyclonal anti-TGF-β1 antibody and rabbit polyclonal anti-type I collagen antibody (1:200; Santa Cruz Biotechnology), rabbit polyclonal anti-type IV collagen antibody (1:200; Santa Cruz Biotechnology), and rabbit polyclonal anti-α-SMA antibody (1:100; Santa Cruz Biotechnology). For coloration, slides were incubated at room temperature with a mixture of 0.05% 3,3´-diaminobenzidine containing 0.01% H_2O_2 and then counterstained with Mayer's hematoxylin. Negative control sections were stained under identical conditions with a buffer solution that was substituted for the primary antibody. A pathologist carried out the histological examinations in a blinded manner.

Statistical analysis

Nonparametric analysis was used because of the small sample size. Results are expressed as mean ± s.e.m. Multiple comparisons were carried out using Wilcoxon's rank-sum tests and the Bonferroni correction. A Kruskal–Wallis test was used to compare more than two groups, followed by a Mann–Whitney U-test, using a microcomputer-assisted program called SPSS for Windows 20.0 (IBM SPSS statistics, Chicago, IL, USA). *P* value < 0.05 was considered statistically significant.

Ethics statement

All experiments were conducted in accordance with the National Institute of Health and guideline after the approval of the Korea University institutional animal care and use committee.

RESULTS

Physical and biochemical parameters of experimental animals

The physical and biochemical parameters for each group of the experimental animals are shown in Table 1. Injection of high dose ADX induced dehydration and cachexia in a previous animal study (12). In our study, ADX administration inhibited weight gain. Mice with ADX-induced nephropathy displayed a significant decrease in body weight compared to the control mice four weeks after an 11 mg/kg injection of ADX. At the time of sacrifice, mice in the ADX injection group had significantly lower body weight than mice in the control group, and LJ1888 administration led to recovery of body weight lost during ADX treatment. The body weight of LJ1888-treated mice was significantly increased compared to that of ADX-injected mice at six weeks, despite no significant changes in daily water and food intake. Although urine volume tended to increase at two weeks and decrease at four weeks after ADX injection compared with control mice, there was no significant difference based on LJ1888 treatment. Kidney weight was significantly lower in ADX-induced nephropathy than in the control group. However, LJ1888 treatment did not induce any significant change in kidney weight. ADX increased the plasma creatinine level significantly, which was improved by LJ1888 treatment.

Effects of LJ1888 administration on urinary excretion of protein and albumin in ADX-induced nephropathy

ADX leads to direct toxic injury of the glomerular filtration barrier including podocytes, the glomerular basement membrane and glomerular endothelial cells. Podocyte damage induces loss of protein and nephrin in the urine (13). In order to investigate the effects of LJ1888 on podocyte injury in ADX-induced nephropathy, we checked the urinary excretion of protein and

Table 1. Physical and biochemical parameters of experimental animals

Parameters	Week	Control (n = 5)	ADX (n = 10)	ADX + LJ1888 (n = 10)
Body weight, g	0	23.20 ± 0.20	23.09 ± 0.41	22.80 ± 0.33
	4	27.20 ± 0.49	24.91 ± 0.37*	25.60 ± 0.40†
	6	29.00 ± 0.32	20.50 ± 1.09*	23.90 ± 1.00*,‡
Daily water intake, g	0	9.00 ± 0.45	5.12 ± 0.57	5.88 ± 0.46
	6	5.60 ± 0.40	6.75 ± 1.25	4.40 ± 0.40
Daily food intake, g	0	4.20 ± 0.20	3.60 ± 0.19	4.02 ± 0.24
	6	4.80 ± 0.37	4.25 ± 1.11	3.60 ± 0.68
Urine volume, mL/d	0	386.00 ± 88.80	238.33 ± 46.51	556.00 ± 78.09
	2	266.00 ± 24.21	414.55 ± 70.60	536.00 ± 83.79†
	4	880.00 ± 296.61	279.50 ± 83.75	316.00 ± 65.71
	6	488.00 ± 63.44	435.00 ± 135.98	232.00 ± 28.00†
Plasma Cr, mg/dL	6	0.075 ± 0.003	0.116 ± 0.009†	0.082 ± 0.007‡
Kidney/100 g Body weight	6	2.575 ± 0.055	1.816 ± 0.077*	1.727 ± 0.050*
Heart/100 g Body weight	6	0.631 ± 0.016	0.643 ± 0.027	0.591 ± 0.018

Values are expressed as (means ± SEM).
ADX, adriamycin; Cr, creatinine.
*P < 0.01; †P < 0.05 vs. control; ‡P < 0.05 vs. ADX.

albumin. Urinary protein excretion was significantly increased at four and six weeks after ADX injection compared with the control group. LJ1888 treatment inhibited urinary protein excretion during two weeks of treatment in ADX-induced nephropathy (Fig. 1A). In addition, urinary albumin excretion significantly increased four and six weeks after ADX injection compared with the control group, and significantly decreased after two weeks of LJ1888 treatment in ADX-induced nephropathy (Fig. 1B).

Effects of LJ1888 on oxidative stress and urinary nephrin excretion in ADX-induced nephropathy

The mechanism of ADX-induced nephropathy occurs in part through podocyte injury via oxidative stress. ADX exacerbates cellular damage in the renal cortex, inducing renal fibrosis (14). Examination of urinary 8-isoprostane excretion and kidney lipid peroxidation (LPO) concentration is an approach for diagnostic assessment of oxidative stress in the kidney (15). In our study, the urinary level of 8-isoprostane markedly increased six weeks after ADX injection compared with the control group, and significantly decreased after two weeks of LJ1888 treatment

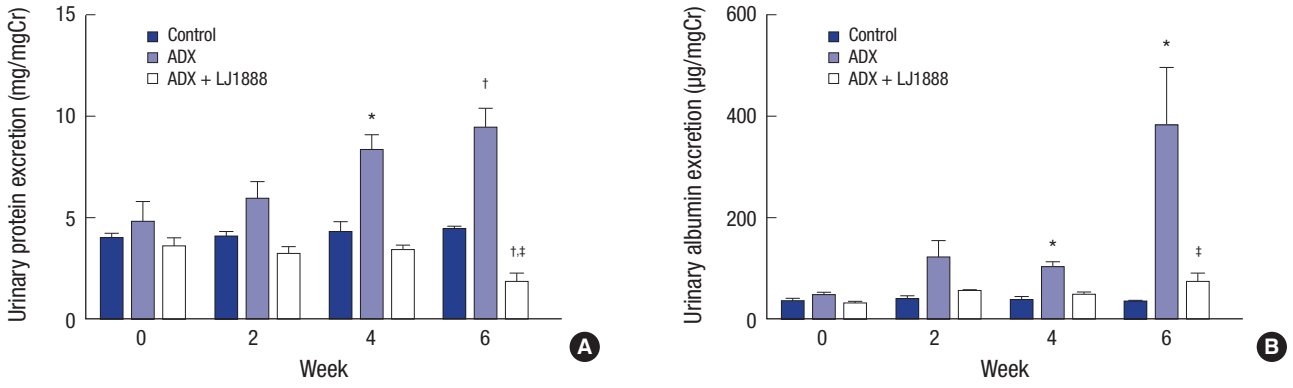

Fig. 1. Effects of LJ1888 on urinary excretion of protein and albumin in experimental ADX-induced nephropathy. (**A**) Twenty-four hour urinary protein excretion level. (**B**) Urinary excretion of albumin level. Urinary protein, albumin, and nephrin levels were corrected for urine creatinine levels.
Values are expressed as (means ± SEM).
ADX, adriamycin.
*$P < 0.01$; †$P < 0.05$ vs. control; ‡$P < 0.001$ vs. ADX.

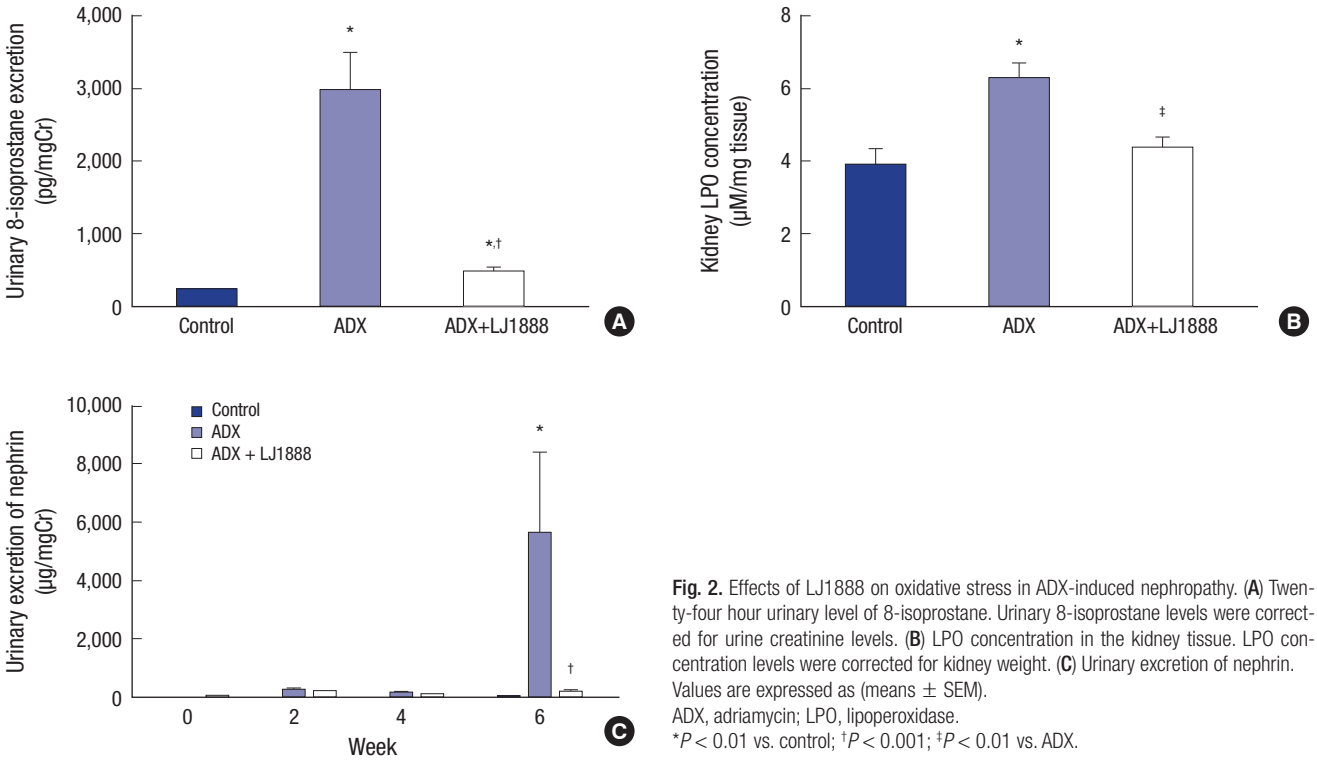

Fig. 2. Effects of LJ1888 on oxidative stress in ADX-induced nephropathy. (**A**) Twenty-four hour urinary level of 8-isoprostane. Urinary 8-isoprostane levels were corrected for urine creatinine levels. (**B**) LPO concentration in the kidney tissue. LPO concentration levels were corrected for kidney weight. (**C**) Urinary excretion of nephrin.
Values are expressed as (means ± SEM).
ADX, adriamycin; LPO, lipoperoxidase.
*$P < 0.01$ vs. control; †$P < 0.001$; ‡$P < 0.01$ vs. ADX.

http://dx.doi.org/10.3346/jkms.2016.31.9.1403

(Fig. 2A). Likewise, LPO concentration in the kidney was significantly increased six weeks after ADX injection compared with the control group, but significantly decreased after LJ1888 treatment (Fig. 2B). In addition, we measured urinary nephrin excretion to determine podocyte injury. As shown in Fig. 2C, each group showed no significant difference in urinary nephrin excretion during four weeks after ADX administration. However, nephrin was markedly increased at six weeks after ADX injection compared with the control group. Interestingly, LJ1888 treatment yielded the greatest inhibitory effects on urinary nephrin excretion.

Effects of LJ1888 on proinflammatory and profibrotic mechanisms in ADX-induced nephropathy

To determine whether LJ1888 has a protective effect in ADX nephropathy, we next investigated the mRNA expression of proinflammatory and profibrotic molecules in renal cortical tissue. Gene expression of profibrotic cytokines including type IV collagen, plasminogen activator inhibitor (PAI)-1, macrophage/monocyte chemoattractant protein (MCP)-1, and NOX4 were remarkably increased in ADX-injected mice. On the other hand, LJ1888 treatment significantly suppressed the expression of PAI-1, MCP-1, and NOX4. TGF-β1 mRNA levels in the renal cortex (Fig. 3A). Similarly, proinflammatory cytokines such as TLR4, tumor necrosis factor (TNFα), interleukin (IL)-1β, and interferon (IFN)-γ were highly expressed after ADX administration compared to the control group, and their mRNA expression was significantly suppressed after LJ1888 treatment. As expected, A3AR mRNA levels significantly increased after ADX injection, but did not change significantly after LJ1888 administration (Fig. 3B). Moreover, western blot analysis confirmed that the renal cortical expression of NF-κB, TGF-β1, and NOX4 were all markedly induced in ADX-injected mice. On the other hand, LJ1888 significantly reduced the expression of all these proteins. TLR4 did not differ among the three groups in the kidney (Fig. 3C).

Effects of LJ1888 on histomorphological changes in ADX-induced nephropathy

Fig. 4 shows representative renal pathology and immunohistochemical staining for each group of experimental animals at the time of sacrifice. PAS and Masson's trichrome staining demonstrated that glomerular and tubulointerstitial damage includ-

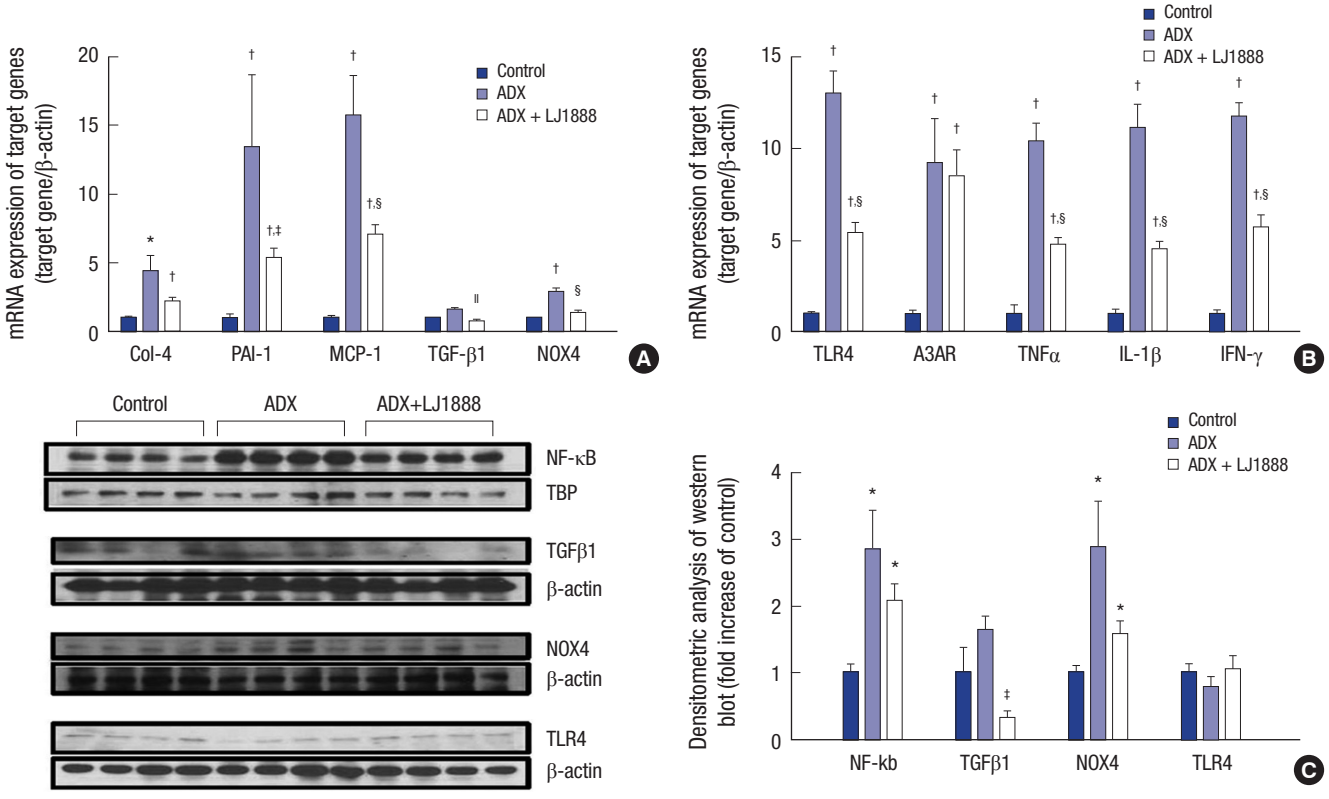

Fig. 3. Effects of LJ1888 on inflammation and fibrosis in ADX-induced nephropathy. (**A** and **B**) Effects of LJ1888 on the expression of inflammatory and fibrotic cytokines. (**C**) Representative western blots of NF-κB, TGF-β1, NOX4, and TLR4 in the kidney and quantitative analysis scoring of western blot.
Values are expressed as (means ± SEM).
ADX, adriamycin; Col-4, type IV collagen; PAI-1, plasminogen activator inhibitor-1; MCP-1, macrophage/monocyte chemoattractant peptide-1; TGF-β1, transforming growth factor-β1; NOX-4, NADPH oxidase 4; TLR-4,Toll-like receptor 4; A3AR, A3 adenosine receptor; TNFα, tumor necrosis α; IL-1β, interleukine-1β; IFN-γ, interferon-γ; NF-κB, nuclear factor-κB.
*$P < 0.05$; †$P < 0.01$ vs. control; ‡$P < 0.05$; §$P < 0.001$; ‖$P < 0.01$ vs. ADX.

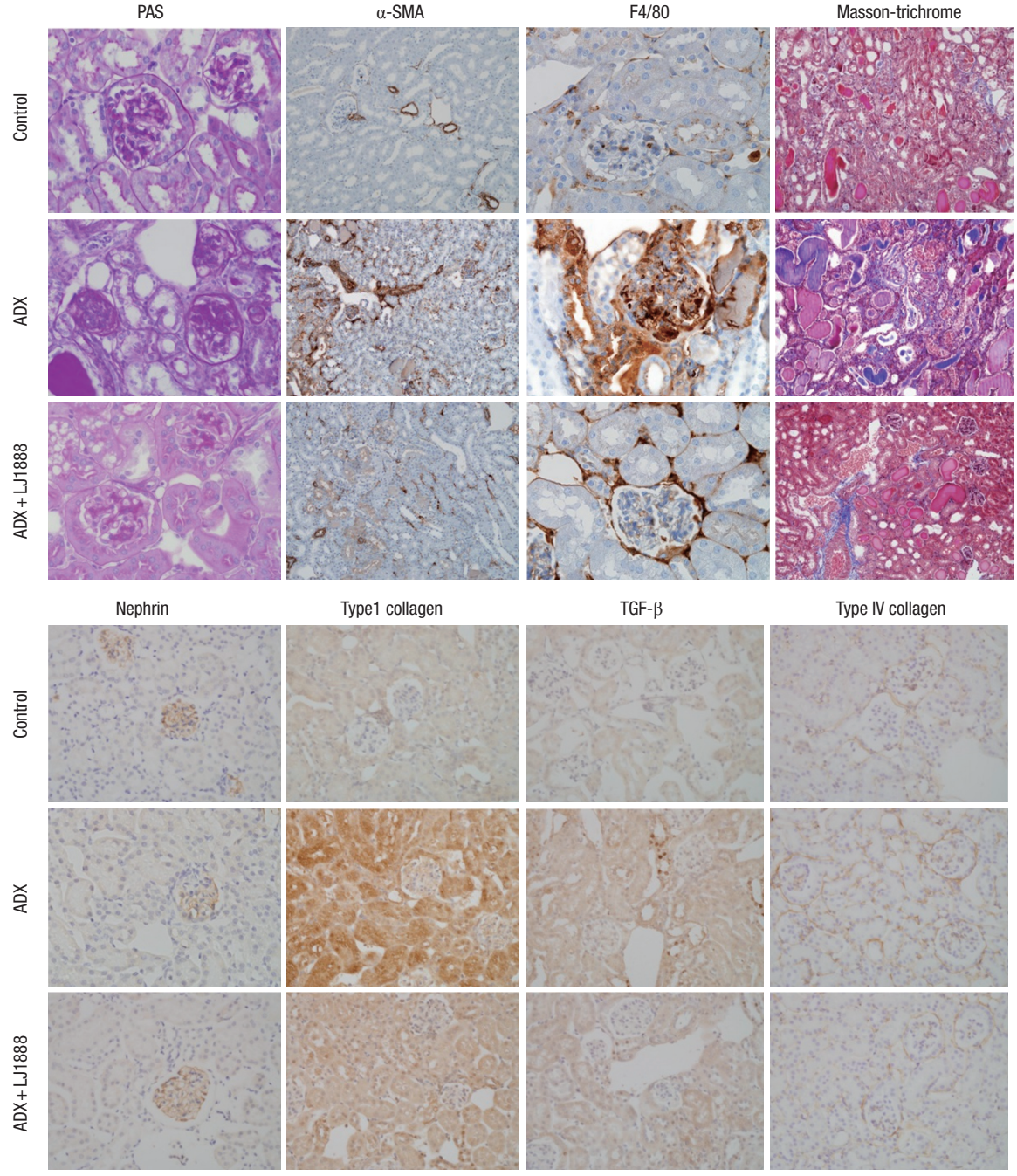

Fig. 4. Representative renal histological and immunohistochemical staining in experimental models at the time of sacrifice. Representative sections show that the histological changes and immunohistochemical staining for PAS, F4/80, Masson's trichrome and α-SMA, nephrin, type I collagen, TGF-β1, and type IV collagen are increased in ADX-induced nephropathy and decreased after treatment with LJ1888. Original magnification × 400.
ADX, adriamycin; PAS, periodic acid-Schiff; α-SMA, α-smooth muscle actin; TGF-β1, transforming growth factor-β1.

ing glomerulosclerosis, excessive collagen deposition, interstitial fibrosis, and tubular atrophy were dramatically increased in ADX-induced nephropathy. The glomeruli had much more severe pathological changes than the tubulointerstitium in ADX-induced nephropathy. ADX led to development of progressive glomerulosclerosis and demonstrated increased accumulation of type I collagen, type IV collagen, TGF-β1, and α-SMA in the glomeruli. In contrast, LJ1888 administration significantly ameliorated severe damage lesions of glomerulosclerosis. Infiltration of inflammatory cells such as macrophages and T lymphocytes in the renal glomeruli is an important pathological finding in the early progression of ADX-induced nephropathy (12). F4/80 is macrophage specific to the inflammatory process. F4/80 staining demonstrated that macrophage infiltration in the glomeruli was markedly increased after ADX injection and dramatically recovered with LJ1888 treatment. Nephrin has important effects

 http://dx.doi.org/10.3346/jkms.2016.31.9.1403

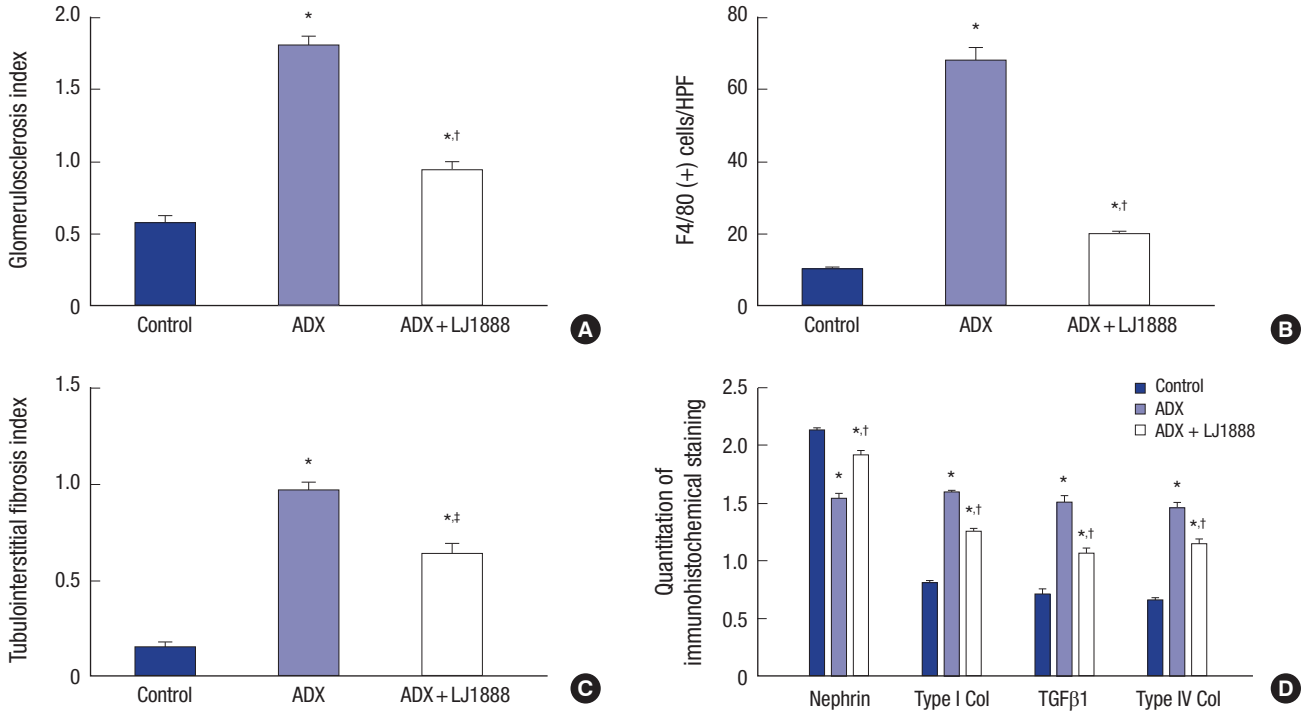

Fig. 5. Quantitation of immunohistochemical staining. (**A**) Glomerulosclerosis index, (**B**) F4/80 positive cell staining score, (**C**) Tubulointerstitial fibrosis index, (**D**) Quantitation of immunohistochemical staining of nephrin, type I Collagen, TGF-β1 and Type 4 collagen.
Values are expressed as (means ± SEM).
ADX, adriamycin.
*$P < 0.01$ vs. control; †$P < 0.001$; ‡$P < 0.01$ vs. ADX.

in controlling the integrity and functions of the podocyte slit diaphragm structure (16). In a previous study, ADX induced direct toxic damage to the podocytes and loss of nephrin in urine (13). Immunohistochemical staining revealed that the numbers of nephrin-positive cells were dramatically decreased in the glomeruli of ADX-injected mice and were significantly restored by LJ1888 treatment. As shown in Fig. 5, quantitative analysis with immunohistochemical staining demonstrated those results.

DISCUSSION

In the present study, we first demonstrated that a highly selective A3AR antagonist reduced proteinuria and albuminuria, improved renal function, and recovered histomorphological changes that occurred during ADX-induced nephropathy. We concluded that this selective A3AR antagonist had a notable effect on urinary nephrin excretion and its glomerular expression, which may prevent podocyte injury. Clinically, proteinuria is the most characteristic manifestation of podocyte injury in kidney disease. We used ADX to develop the renal glomerular injury. ADX induces proteinuria and nephrin loss in urine by injuring the glomerular filtration barrier, decreasing glomerular endothelial cell thickness and glomerular charge selectivity and increasing podocyte foot process effacement (17,18). The renal histological changes due to ADX appear about one week after ADX administration and degenerate into severe injury by four weeks (19).

Adenosine has various effects in the kidneys, including the regulation of renin secretion, glomerular filtration rate, renal vascular tone, tubular glomerular feedback, fluid and electrolyte transport of the tubular and collecting duct system, and metabolic renal function. The concentration of extracellular adenosine is maintained at approximately 100 nM under normal conditions and rapidly increases during renal cell damage (20). A previous study demonstrated that long-term exposure to high concentrations of adenosine induced secretion of intracellular proinflammatory cytokines, activation of fibroblasts, and deposition of collagen in the extracellular matrix (21). A recent study showed that an increase in adenosine levels led to ischemic renal fibrosis and finally induced renal interstitial fibrosis in renal cell damage in the unilateral ureteral obstruction model (22).

Activation of A3AR by adenosine leads to a decrease in adenylyl cyclase activity and cAMP production, which induce stimulation of phospholipase C (PLC) activity, Ca2+ mobilization, and phosphorylation of phosphatidylinositol 3-kinase (PI3K) and AKT. AKT modulates the mitogen-activated protein kinase (MAPK) family including c-JUN N-terminal kinase (JNK), extracellular signal-regulated kinase (ERK), and p38 MAPK (6). There-

fore, A3AR activation stimulates p38 MAPK phosphorylation, leading to decreased hypoxic damage of cardiomyocytes (23). On the other hand, A3AR activation suppresses the p38 MAPK pathway, leading to down-regulation of the inflammatory status in human synoviocytes (24). A3AR has different effects in different cell types, such as cell proliferation and cell death, which may be related to PI3K/AKT and ERK1/2 pathway crosstalk (25). Many studies have shown the biologic functions and therapeutic applications of A3AR and A3AR antagonists in the brain, heart, lung, and immune system (6).

LJ1888 dramatically suppressed the urinary excretion of nephrin. In immunohistochemical staining, the numbers of nephrin-positive cells were dramatically decreased by ADX and significantly restored by LJ1888 treatment. Nephrin is one of the molecules that constitute the podocyte slit diaphragm and it is involved the maturation of podocytes during glomerular development (26). Nephrin induces phosphorylation and activation of the PI3K-dependent AKT downstream signaling pathway. Several AKT targets bind to the phosphorylation-dependent 14-3-3 proteins, which are involved in the control of cell growth, migration, proliferation, and apoptosis. Nephrin-induced PI3K/AKT signaling plays a preventative role in podocyte apoptosis (27). A3AR transmits a cellular proliferation signal through the PI3K/AKT signaling pathway. Stimulated AKT is able to phosphorylate many downstream substrates such as Raf. Therefore, by blocking Raf through AKT activation and inducing cell death, A3AR inhibits the MAPK pathway, including RAS, Raf, MEK1/2, and ERK1/2 (25). A3AR gene expression in renal cortical tissue was dramatically increased in ADX-induced nephropathy. Although LJ1888 did not suppress A3AR gene expression, LJ1888 inhibited A3AR-associated PI3K/AKT and RAS/RAF/MEK/ERK downstream pathways, protecting podocytes from apoptosis. Additional studies are required to demonstrate the interaction of A3AR and nephrin downstream pathways.

There is a considerable body of evidence regarding oxidative stress in various kidney diseases. In ADX-induced nephropathy, oxidative stress and inflammation are important mechanisms of progressive proteinuric nephropathy leading to renal fibrosis (13). Renal tissue hypoxia induces the elevation of adenosine levels, leading to renal fibrosis (22). Oxidative stress induces stimulation of TGF-β1 expression and production of extracellular matrix, leading to glomerular and tubulointerstitial fibrosis. The MAPK family signaling is activated by oxidative stress in renal cells. The JNK pathway is associated with progression of renal fibrosis and tubular apoptosis (28). Stimulation of the ERK pathway is related to proliferative glomerulonephritis (29). Activation of the p38 MAPK pathway by IL-1, TNF-α, and TFG-β1 induces extracellular matrix accumulation, leading to tubulointerstitial fibrosis (30). A previous study demonstrated that LJ1888 significantly suppressed JNK and ERK phosphorylation during TGF-β1 upregulation in the kidney (9). In this study, we observed that LJ1888 treatment attenuated the increased urinary excretion of 8-isoprostane and the increased LPO concentration in kidney tissue after ADX injection.

In addition, mRNA expression of proinflammatory molecules including TLR4, TNFα, IL-1β, and IFN-γ increased in ADX-induced nephropathy, and dramatically recovered during LJ1888 treatment. The TLR4/NK-κB pathway is considered to be an important link between inflammation and oxidative stress in kidney disease (31,32). Gene expression of profibrotic molecules including type IV collagen, PAI-1, MCP-1, TGF-β1, and NOX4, as wells as NF-κB protein, were increased by ADX and significantly decreased by LJ1888. Renal histological and immunohistochemical staining demonstrated similar results consistently. Type I collagen, type IV collagen, TGF-β1, and α-SMA accumulation in the fibrotic area of the renal glomeruli were increased in ADX-induced nephropathy, as was macrophage infiltration. Those profibrotic and proinflammatory molecules were genetically suppressed significantly by LJ1888 administration. The extensive glomerular and tubulointerstitial damage, including glomerulosclerosis, excessive collagen deposition, interstitial fibrosis, and tubular atrophy, were dramatically increased in ADX-induced nephropathy. In contrast, LJ1888 administration significantly ameliorated severe damage lesions in both the glomerular and tubular compartments. We suggest that LJ 1888 ameliorated oxidative stress, inflammation, and fibrosis in ADX-induced nephropathy through antioxidative mechanisms via A3AR.

In summary, we are the first to show that LJ1888, a highly selective A3AR antagonist, exhibits renoprotective effects by ameliorating podocyte injury, oxidative stress, inflammation, glomerulosclerosis, and tubulointerstitial fibrosis in ADX-induced nephropathy. Treatment with LJ1888 induced renoprotective effects by attenuating podocyte injury through decreased urinary excretion of nephrin. Therefore, we suggest that LJ1888 could be a new therapeutic drug for proteinuric renal disease. We recommend further study of LJ1888 in progressive renal disease to demonstrate its therapeutic effect more clearly.

DISCLOSURE

The authors have no potential conflicts of interest to disclose.

AUTHOR CONTRIBUTION

Research conception & design: Min HS, Cha JJ, Kang YS. Performing the experiments: Min HS, Kim JE, Ghee JY, Jeong LS. Data acquisition: Kim JE, Min HS, Cha JJ, Cha DR. Data analysis and interpretation: Han JY, Cha DR, Kang YS. Statistical analysis: Min HS, Cha JJ, Kang YS. Drafting of the manuscript: Min HS, Cha JJ. Critical revision of the manuscript: Min HS, Cha JJ, Kim HW, Lee JE, Kang YS. Receiving grant: Kang YS, Cha DR.

http://dx.doi.org/10.3346/jkms.2016.31.9.1403

Approval of final manuscript: all authors.

ORCID

Hye Sook Min http://orcid.org/0000-0002-9576-6054
Jin Joo Cha http://orcid.org/0000-0001-6779-0113
Kitae Kim http://orcid.org/0000-0003-2433-1747
Jung Eun Kim http://orcid.org/0000-0002-5260-7563
Jung Yeon Ghee http://orcid.org/0000-0002-5817-237X
Hyunwook Kim http://orcid.org/0000-0002-4274-7562
Ji Eun Lee http://orcid.org/0000-0002-8299-4816
Jee-Young Han http://orcid.org/0000-0003-3224-4029
Lak Shin Jeong http://orcid.org/0000-0002-3441-707X
Dae Ryong Cha http://orcid.org/0000-0003-0063-2844
Young Sun Kang http://orcid.org/0000-0002-4061-386X

REFERENCES

1. Vallon V, Mühlbauer B, Osswald H. Adenosine and kidney function. *Physiol Rev* 2006; 86: 901-40.
2. Hirschhorn R, Roegner-Maniscalco V, Kuritsky L, Rosen FS. Bone marrow transplantation only partially restores purine metabolites to normal in adenosine deaminase-deficient patients. *J Clin Invest* 1981; 68: 1387-93.
3. Cronstein BN, Naime D, Firestein G. The antiinflammatory effects of an adenosine kinase inhibitor are mediated by adenosine. *Arthritis Rheum* 1995; 38: 1040-5.
4. Jacobson KA, Gao ZG. Adenosine receptors as therapeutic targets. *Nat Rev Drug Discov* 2006; 5: 247-64.
5. Brandon CI, Vandenplas M, Dookwah H, Murray TF. Cloning and pharmacological characterization of the equine adenosine A3 receptor. *J Vet Pharmacol Ther* 2006; 29: 255-63.
6. Borea PA, Varani K, Vincenzi F, Baraldi PG, Tabrizi MA, Merighi S, Gessi S. The A3 adenosine receptor: history and perspectives. *Pharmacol Rev* 2015; 67: 74-102.
7. Lee HT, Emala CW. Protective effects of renal ischemic preconditioning and adenosine pretreatment: role of A(1) and A(3) receptors. *Am J Physiol Renal Physiol* 2000; 278: F380-7.
8. Lee HT, Ota-Setlik A, Xu H, D'Agati VD, Jacobson MA, Emala CW. A3 adenosine receptor knockout mice are protected against ischemia- and myoglobinuria-induced renal failure. *Am J Physiol Renal Physiol* 2003; 284: F267-73.
9. Lee J, Hwang I, Lee JH, Lee HW, Jeong LS, Ha H. The selective A3AR antagonist LJ-1888 ameliorates UUO-induced tubulointerstitial fibrosis. *Am J Pathol* 2013; 183: 1488-97.
10. Jeong LS, Choe SA, Gunaga P, Kim HO, Lee HW, Lee SK, Tosh DK, Patel A, Palaniappan KK, Gao ZG, et al. Discovery of a new nucleoside template for human A3 adenosine receptor ligands: D-4'-thioadenosine derivatives without 4'-hydroxymethyl group as highly potent and selective antagonists. *J Med Chem* 2007; 50: 3159-62.
11. Lee MH, Song HK, Ko GJ, Kang YS, Han SY, Han KH, Kim HK, Han JY, Cha DR. Angiotensin receptor blockers improve insulin resistance in type 2 diabetic rats by modulating adipose tissue. *Kidney Int* 2008; 74: 890-900.
12. Wang Y, Wang YP, Tay YC, Harris DC. Progressive adriamycin nephropathy in mice: sequence of histologic and immunohistochemical events. *Kidney Int* 2000; 58: 1797-804.
13. Szalay CI, Erdélyi K, Kökény G, Lajtár E, Godó M, Révész C, Kaucsár T, Kiss N, Sárközy M, Csont T, et al. Oxidative/nitrative stress and inflammation drive progression of doxorubicin-induced renal fibrosis in rats as revealed by comparing a normal and a fibrosis-resistant rat strain. *PLoS One* 2015; 10: e0127090.
14. Deman A, Ceyssens B, Pauwels M, Zhang J, Houte KV, Verbeelen D, Van den Branden C. Altered antioxidant defence in a mouse adriamycin model of glomerulosclerosis. *Nephrol Dial Transplant* 2001; 16: 147-50.
15. Montuschi P, Barnes PJ, Roberts LJ 2nd. Isoprostanes: markers and mediators of oxidative stress. *FASEB J* 2004; 18: 1791-800.
16. Machado JR, Rocha LP, Neves PD, Cobô Ede C, Silva MV, Castellano LR, Corrêa RR, Reis MA. An overview of molecular mechanism of nephrotic syndrome. *Int J Nephrol* 2012; 2012: 937623.
17. Jeansson M, Björck K, Tenstad O, Haraldsson B. Adriamycin alters glomerular endothelium to induce proteinuria. *J Am Soc Nephrol* 2009; 20: 114-22.
18. Fujimura T, Yamagishi S, Ueda S, Fukami K, Shibata R, Matsumoto Y, Kaida Y, Hayashida A, Koike K, Matsui T, et al. Administration of pigment epithelium-derived factor (PEDF) reduces proteinuria by suppressing decreased nephrin and increased VEGF expression in the glomeruli of adriamycin-injected rats. *Nephrol Dial Transplant* 2009; 24: 1397-406.
19. Lee VW, Harris DC. Adriamycin nephropathy: a model of focal segmental glomerulosclerosis. *Nephrology (Carlton)* 2011; 16: 30-8.
20. Vallon V, Osswald H. Adenosine receptors and the kidney. In: Wilson CN, Mustafa SJ, editors. Adenosine Receptors in Health and Disease. Dordrecht: Springer, 2009, p443-70.
21. Dai Y, Zhang W, Wen J, Zhang Y, Kellems RE, Xia Y. A2B adenosine receptor-mediated induction of IL-6 promotes CKD. *J Am Soc Nephrol* 2011; 22: 890-901.
22. Tang J, Jiang X, Zhou Y, Xia B, Dai Y. Increased adenosine levels contribute to ischemic kidney fibrosis in the unilateral ureteral obstruction model. *Exp Ther Med* 2015; 9: 737-43.
23. Leshem-Lev D, Hochhauser E, Chanyshev B, Isak A, Shainberg A. Adenosine A(1) and A (3) receptor agonists reduce hypoxic injury through the involvement of P38 MAPK. *Mol Cell Biochem* 2010; 345: 153-60.
24. Varani K, Vincenzi F, Tosi A, Targa M, Masieri FF, Ongaro A, De Mattei M, Massari L, Borea PA. Expression and functional role of adenosine receptors in regulating inflammatory responses in human synoviocytes. *Br J Pharmacol* 2010; 160: 101-15.
25. Merighi S, Benini A, Mirandola P, Gessi S, Varani K, Leung E, Maclennan S, Baraldi PG, Borea PA. Modulation of the Akt/Ras/Raf/MEK/ERK pathway by A3 adenosine receptor. *Purinergic Signal* 2006; 2: 627-32.
26. Doné SC, Takemoto M, He L, Sun Y, Hultenby K, Betsholtz C, Tryggvason K. Nephrin is involved in podocyte maturation but not survival during glomerular development. *Kidney Int* 2008; 73: 697-704.
27. Huber TB, Hartleben B, Kim J, Schmidts M, Schermer B, Keil A, Egger L, Lecha RL, Borner C, Pavenstädt H, et al. Nephrin and CD2AP associate with phosphoinositide 3-OH kinase and stimulate AKT-dependent signaling. *Mol Cell Biol* 2003; 23: 4917-28.
28. Ma FY, Flanc RS, Tesch GH, Han Y, Atkins RC, Bennett BL, Friedman GC, Fan JH, Nikolic-Paterson DJ. A pathogenic role for c-Jun amino-terminal kinase signaling in renal fibrosis and tubular cell apoptosis. *J Am Soc Nephrol* 2007; 18: 472-84.

29. Pat B, Yang T, Kong C, Watters D, Johnson DW, Gobe G. Activation of ERK in renal fibrosis after unilateral ureteral obstruction: modulation by antioxidants. *Kidney Int* 2005; 67: 931-43.
30. Stambe C, Atkins RC, Tesch GH, Masaki T, Schreiner GF, Nikolic-Paterson DJ. The role of p38α mitogen-activated protein kinase activation in renal fibrosis. *J Am Soc Nephrol* 2004; 15: 370-9.
31. Min HS, Kim JE, Lee MH, Song HK, Lee MJ, Lee JE, Kim HW, Cha JJ, Hyun YY, Han JY, et al. Effects of Toll-like receptor antagonist 4,5-dihydro-3-phenyl-5-isoxasole acetic acid on the progression of kidney disease in mice on a high-fat diet. *Kidney Res Clin Pract* 2014; 33: 33-44.
32. Mkaddem SB, Bens M, Vandewalle A. Differential activation of toll-like receptor-mediated apoptosis induced by hypoxia. *Oncotarget* 2010; 1: 741-50.

http://dx.doi.org/10.3346/jkms.2016.31.9.1403

Supplementary Table 1. Primer sequences for real-time quantitative PCR

Target genes	Primer sequences (´5-´3)
TLR4, forward	GGGAACAAACAGCCTGAGAC
TLR4, reverse	AGACCCATGAAATTGGCA T
TNF-α, forward	CCGATGGGTTGTACCTTGTC
TNF-α, reverse	GGCAGAGAGGAGGTTGACTTT
IL-1β, forward	CTC ACA AGC AGA GCA CAA GC
IL-1β, reverse	ACG GAT TCC ATG GTG AAG TC
MCP-1, forward	CTGGATCGGAACCAAATGAG
MCP-1, reverse	CGGGTCAACTTCACATTCAA
PAI-1, forward	TCCTCATCCTGCCTAAGTTCTC
PAI-1, reverse	GTGCCGCTCTCGTTTACCTC
TGF-β1, forward	AGCCCGAAGCGGACTACTAT
TGF-β1, reverse	CTGTGTGAGATGTCTTTGGTTTTC
Col-IV, forward	GCTCTGGCTGTGGAAAATGT
Col-IV, reverse	CTTGCATCCCGGGAAATC
A3AR, forward	CTCTTCTTGTTTGCGCTGTG
A3AR, reverse	GCACATTGCGACATCTGGT
IFN-γ, forward	GCGTCATTGAATCACACCTG
IFN-γ, reverse	TGAGCTCATTGAATGCTTGG
NOX4, forward	TTGGTGAATGCCCTCAACTT
NOX4, reverse	TTCTGGGATCCTCATTCTGG
β-actin, forward	GGACTCCTATGTGGGTGACG
β-actin, reverse	CTTCTCCATGTCGTCCCAGT

In this experiment, each sample was run in triplicate, and the corresponding non-reverse transcribed mRNA samples were used as negative controls. The mRNA level of each sample was normalized to that of β-actin mRNA.
TLR4, Toll like receptor 4; TNF-α, Tumor necrosis factor-α; IL-1, interleukin-1; MCP-1, monocyte chemoattractant peptide-1; PAI-1, plasminogen activator inhibitor-1; TGF-β1, transforming growth factor; Col-IV, type IV collagen; A3AR, A3 adenosine receptor; IFN-γ, interferon; NOX4, NADPH oxidase 4.